Seasonal Tropical Cyclone Activity Forecast Northwest Pacific Ocean and South China Sea | March 2026

I. Forecasting Results

It is forecasted that in 2026, the genesis frequency of tropical storms (TS) over the Northwest Pacific and the South China Sea will **below normal to near normal LTCA (Long-Term Climate Average),** approximately 23-25 in total. The frequency of super typhoon (STY) will be slightly below normal LTCA, approximately 7–9. The frequency of TS making landfall in China will be near the LTCA, approximately 6–8.

The frequency of TC that affecting China in 2026 is forecasted to be **at the LTCA**, approximately 12–14 in total. The frequency of TC affecting South China and East China are forecasted to be above normal to near normal than LTCA, approximately 9-11 for each region; while the frequency of TC affecting areas in the vicinity of Shanghai is close to the LTCA (approximately 2).

Table 1. Seasonal forecast of TC activity in 2026

	Event Genesis		Landfall	TC Affecting China (see Notes 1-2)			
	(>=TS)	(>=STY)	(>=TS)	Countrywide	South	East	Shanghai
1991-2020 EV ± SD	25±4.5	9.5±3.6	7±1.9	13.0±3.6	9.0±3.5	9.5±3.3	2.0±1.5
2026 Early Season Forecast	23-25	7-9	6-8	12-14	9-11	9-11	~2

II. Basis for forecasting

1. Ocean Atmosphere Conditions and Outlook

As of February 2026, sea surface temperatures (SSTs) over the central and eastern equatorial Pacific remain as weak negative anomalies, while weak positive anomalies are observed over the western Pacific (Figure 1). During November 2025 to January 2026, SSTs in the Niño3.4 were maintained below −0.5 °C. More recently, negative SST anomalies in the central and eastern equatorial Pacific have shown signs of weakening, indicating a gradual weakening of the La Niña events that prevailed during the preceding winter. In contrast, negative SST anomalies over the central and eastern Indian Ocean and the Maritime Continent have shown a tendency of expansion, and SSTs over the Bay of Bengal have gradually transitioned to negative anomalies.

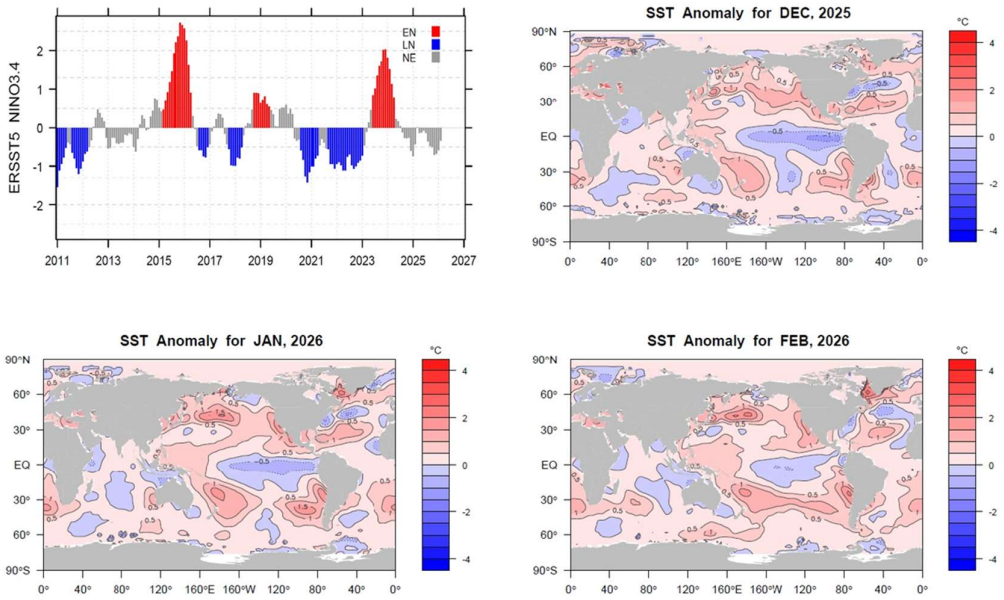

Figure 1. Evolution of the Niño3.4 SST index (upper left panel) and distribution of SST anomalies during December 2025 to February 2026 (upper right, lower left and lower right panels).

Since November 2025, anomalous cyclonic circulation has developed over the tropical regions in the Northwest Pacific, accompanied by a subtropical high weaker than the LTCA with an enhanced and continuous convective activity. These conditions have been favourable for the genesis of one TC per month over the Northwest Pacific during January to March 2026 (Figure 2).

Forecasts from major domestic and international climate centres indicate that the ongoing La Niña event is likely to terminate in the near term (Figure 3). Thereafter, the tropical Pacific is forecasted to remain in a neutral state for a period, before transitioning into El Niño events in late spring or early summer, or even later. Nevertheless, there remains a non-negligible likelihood that neutral states may persist.

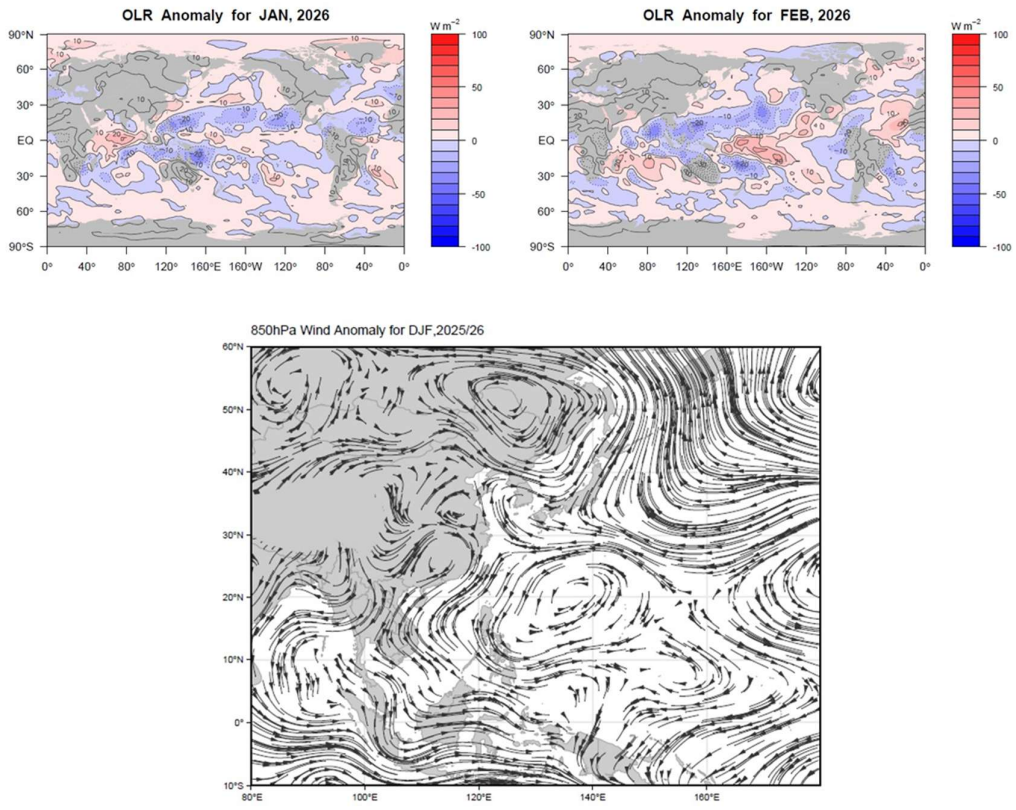

Figure 2. OLR anomalies during January – February 2026 (upper left and upper right panels) and anomalous 850-hPa wind fields distribution for winter 2025/26 (DJF) (lower panel).

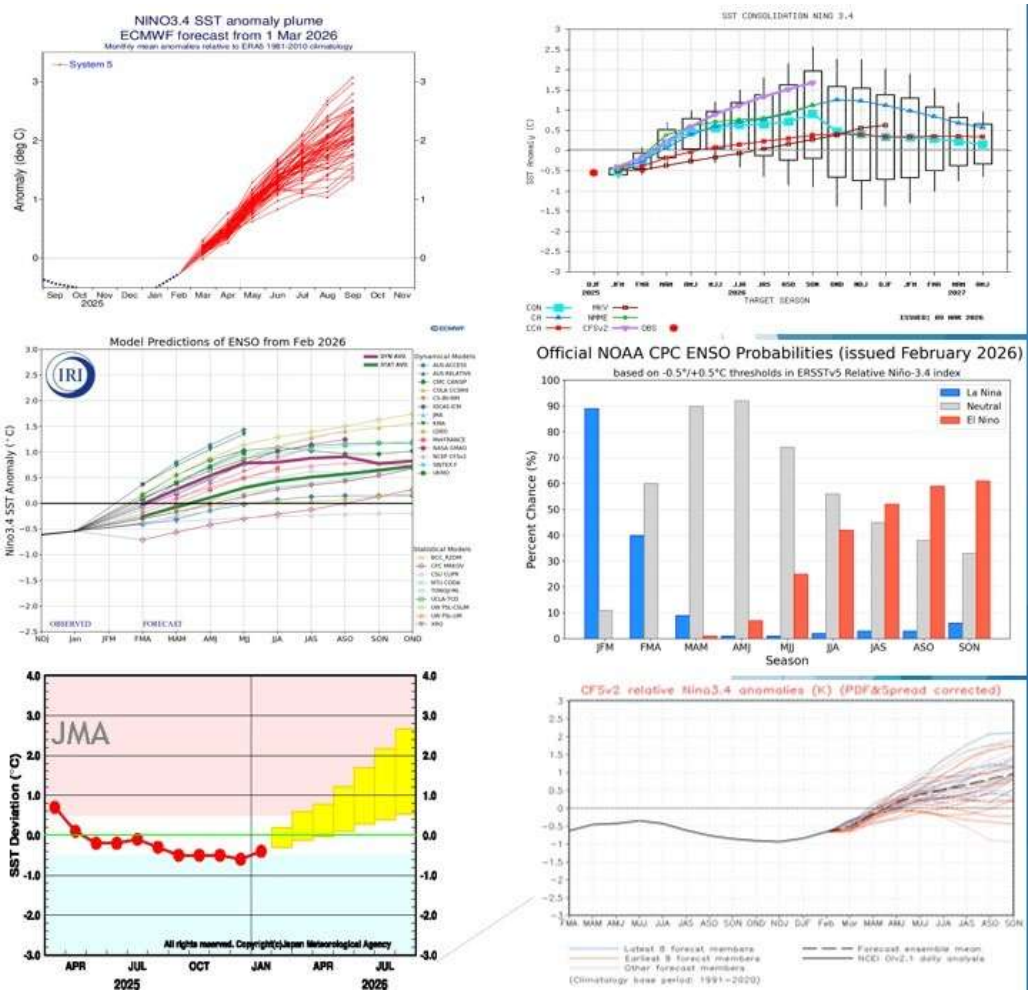

Figure 3. Forecasts of Niño-3.4 sea surface temperature anomalies for 2026 from major climate centres (Japan uses the Niño-3).

Forecasts utilizing the CFSv2 dynamic model indicate that from spring to autumn, geopotential heights are anomalously high over the Indochina Peninsula and the Maritime Continent, suggesting conditions that are generally unfavourable for convective system development in these regions. However, no pronounced anomalies are observed in the core region of the subtropical high (Figure 4).

Forecasts based on the ECMWF model demonstrate a broadly consistent signal: from spring to autumn, sea-level pressure is higher than the LTCA over the Indochina Peninsula and the Maritime Continent, while sea-level pressure over the core region of the Pacific subtropical high is lower than the LTCA. This configuration suggests that regions favourable for TC activity may be displaced relatively eastward.

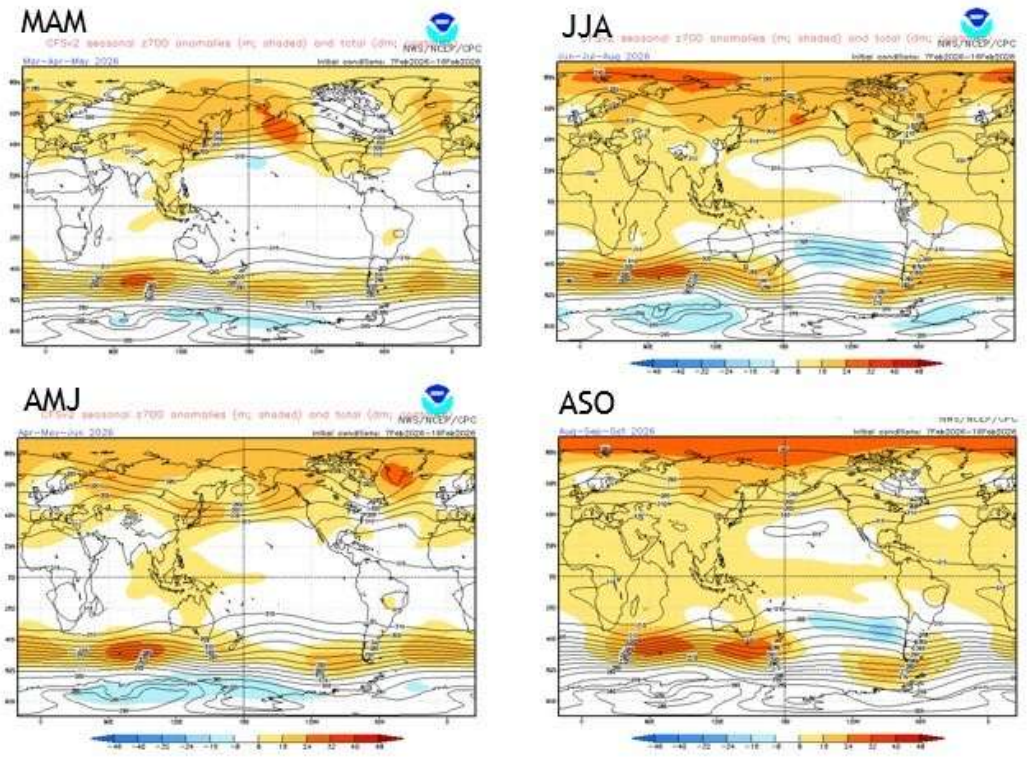

Figure 4. 700-hPa geopotential height anomalies forecast by the U.S. CFSv2 for 2026 (MAM: March–May; AMJ: April–June; JJA: June–August; ASO: August–October).

Seasonal TC forecasts from ECMWF further indicate that TC activity during April–September is projected to be slightly above the LTCA, with an increased frequency of TS (at the 5% significance level), and a marginally higher frequency of TY, (not statistically significant). Moreover, TC tracks show a tendency of north-westward motion affecting East China, with westward-moving and recurving tracks also indicated, though these signals are not statistically significant.

2. ENSO Evolution and Tropical Cyclone Activity in Historical Analogue Years

Utilizing four Niño-region indices for analogue analysis, the years identified as most similar to the period from March 2025 to February 2026 (12 months in total) are 1959, 1960, 2002, and 2018. The evolution of the Niño-3.4 SST index for these analogue years is shown in Figure 5, and the corresponding TC activity statistics are summarized in Table 2. Among the four analogue years, the events transitioned to La Niña by July during the latter stage of 1959. In contrast, neutral conditions persisted through the latter part of 1960. Meanwhile, El Niño events developed during early summer in 2002 and during autumn in 2018, variation in the timing of transitions.

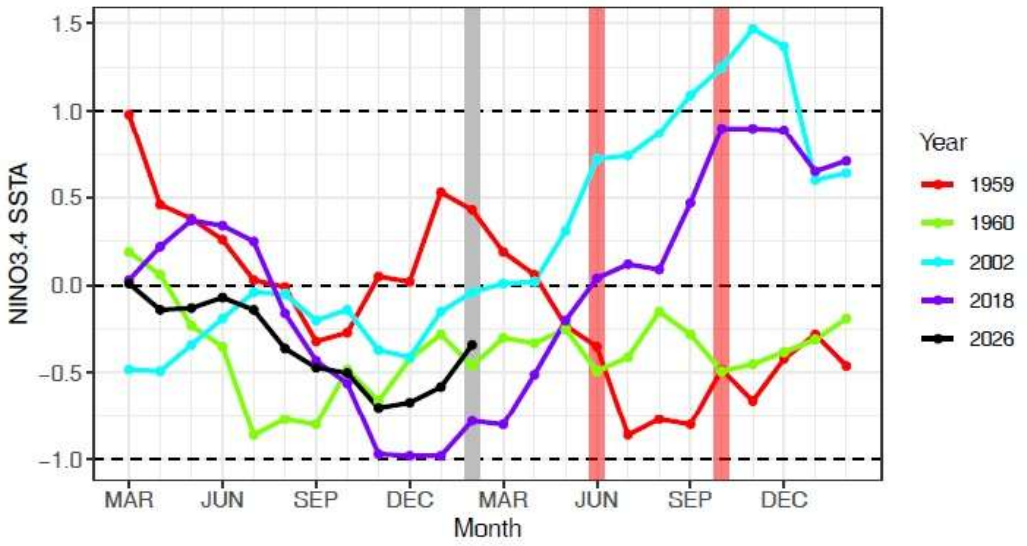

Figure 5. Evolution of the Niño-3.4 SST index in analogue years (1959, 1960, 2002 and 2018).

Table 2. TC activity statistics for ENSO analogue years (EN: El Niño; LN: La Niña; NE: Neutral).

ENSO Evolution	Analogous Years	EN State	Subsequent LN	TS Cyclogenesis	STY	TS landing	Impact Countrywide	Impact South China	Impact East China	Impact Shanghai
Evolves into LN	1959	NE	Evolves into LN in July	23	16	6	16	9	12	5
Remains NE	1960	NE	NE	33	13	6	17	14	10	5
Evolves into EN	2002	NE	Evolves into LN in June	26	13	5	10	6	7	1
	2018	LN Ends in April	Evolves into EN in October	28	11	10	19	12	16	6
Climatological mean ± SD of TC frequency				25±4.5	9.5±3.6	7±1.9	13.0±3.6	9.0±3.5	9.5±3.3	2.0±1.5

As shown in Table 2, the four analogue years display significant differences in ENSO evolution, accompanied by corresponding variations in TC activity. On average, the frequency of TS genesis and landfall is close to the LTCA, while the frequency of STY is above the LTCA. The frequency of TCs affecting overall China, as well as South China and East China, is slightly higher than the LTCA, whereas the frequency of TCs affecting areas near Shanghai is above the LTCA.

A comparison of circulation patterns during summer and autumn across the four analogue years (figures not shown) reveals notable common features despite differences in ENSO evolution. From spring to autumn, all four years exhibit anomalous cyclonic circulation over the eastern region of the Philippines. In 2002 and 2018, the cyclonic anomalies extended further westward into eastern China, forming circulation conditions conducive to TC activity.

These regional circulation characteristics are broadly consistent with the circulation anomalies forecasted by the climate model forecasts for the upcoming summer and autumn. Accordingly, TC activity observed during the analogue years provides a useful reference for the current outlook.

3. Changes in Tropical Cyclone Activity

In 2025, a total of 28 TS genesis over the Northwest Pacific and the South China Sea. Both TS genesis and landfall frequencies were above the LTCA (Figures 6a–b). From a moving-average perspective, TS genesis and landfall frequencies in recent years have entered a transition phase from lower frequencies to higher frequencies (Figures 6a–b). By contrast, the annual frequencies of TCs affecting overall China, East China, and areas near Shanghai shows a transition from higher to lower, while the frequency of TCs affecting South China remains above LTCA (Figures 6c–f).

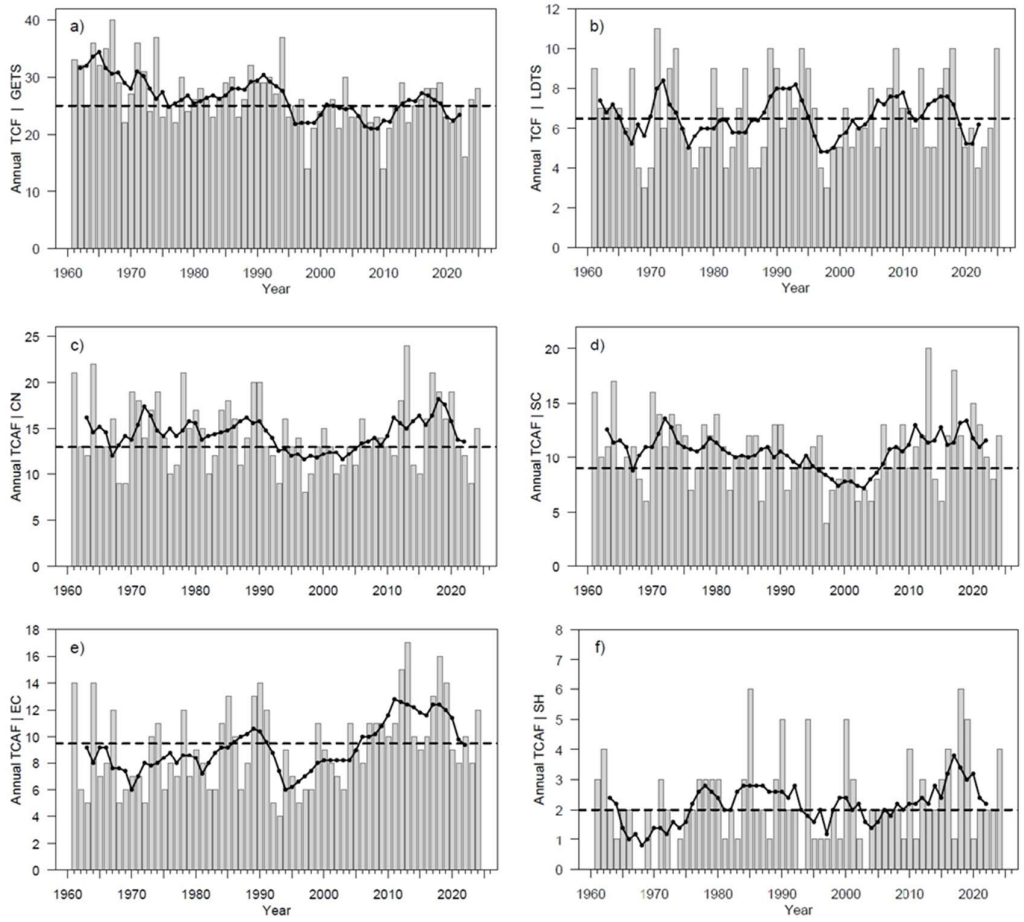

Figure 6. TS genesis over the Northwest Pacific and South China Sea (a), TS landfalls in China (b), TCs affecting China (c), South China (d), East China (e), and areas near Shanghai (f). Annual frequencies are shown as bars, climatological means as dashed lines, and 5-year moving average as lines with dots. TC impact frequency series in panels (c–f) until 2024.

During January – March 2026, three TCs genesis over the east Philippines Sea in the Northwest Pacific (Figure 7), including Severe Tropical Storm Nokaen (2601) on 15 January, Tropical Storm Penha (2602) on 4 February, and Tropical Storm Nuri (2603) on 11 March. As discussed above, anomalous cyclonic circulation over tropical regions in the Northwest Pacific during the preceding winter, along with enhanced convective activity, provided a favourable regional scale background for TC genesis, contributing to the formation of these three systems.

Figure 7. Tropical Cyclones No. 1–3 (2026)

4. Objective Methods and Regional Model Forecast Results

4.1. Deterministic Forecasts Based on Statistical Models

Statistical forecasts were produced using three approaches. The first approach applies a mean-generating function model based on the intrinsic characteristics of the historical time series. The second approach constructs regression models using ocean–atmosphere environmental fields that exhibit strong relationships with the forecast targets. In addition, several machine-learning methods were applied, and the forecast results from different models were ensembled.

The results from these forecasting models are summarized in Table 3. Overall, TS genesis in 2026 is projected to be comparatively lower, while TS landfall frequency is forecasted to be close to the LTCA. The frequency of TCs affecting overall China is forecast to be normal compared to previous years. TC affecting South China and East China are forecasted to slightly above the LTCA, whereas TC affecting areas near Shanghai are expected to be close to the LTCA.

Table 3. Forecast results of annual tropical cyclone frequencies for 2026 based on Statistical model

	TS Genesis	TS Landfall	TC Affecting China (Notes 1-2)			
			Countrywide	South	East	Shanghai
1991-2020 EV ± SD	25±4.5	7±1.9	13.0±3.6	9.0±3.5	9.5±3.3	2.0±1.5
2026 Forecast (Regressive Mean Generating Function)	27 24/23	5.5 7.4/6.5	12.4 12.6	10.2 10.5	7.0 11.3	2.0 2.0
2026 Forecast (Machine Learning Ensemble)	23.3	7.6	14.4	10.7	9.5	1.8

4.2. Hybrid Dynamic–Statistical Model Prediction

Using forecasts of sea surface temperature anomalies during spring-summer 2026, as well as the vertical wind shear and low-level vorticity from the NCEP/CFS system, combining with statistical models constructed on the basis of relationship between key regional factors and TS activity, a hybrid dynamic–statistical prediction is performed. An ensemble is formed from 28 samples initialized in January (00:00, 06:00, 12:00, and 18:00 UTC runs on 1, 6, 11, 16, 21, 26, and 31 January) and 32 samples initialized in February-March (00:00, 06:00, 12:00, and 18:00 UTC runs on 5, 10, 15, 20, and 25 February, and 2, 7, and 12 March). Using this ensemble, both deterministic and probabilistic forecasts of TS and STY frequencies are produced for forecasts initialized in January and in February–March.

The deterministic forecast results are shown in Table 4. Both the annual total and the typhoon-season total (from April to December) of TS genesis frequency in 2026 are projected to be lower than the LTCA, and the STY frequency is also forecasted to be comparatively lower. The probabilistic forecasts from the model (Figure 8) yield consistent results: for the 2026 typhoon season, the forecasts suggest a higher likelihood of below-normal TS genesis frequency, whereas STY frequency is projected to fall within the range between normal and below-normal.

Table 4. Ensemble forecast results for 2025 based on the hybrid dynamic–statistical model

2026 Forecast	Reporting month	Jan	Feb - Mar	1991-2020 EV ± SD
TS Genesis	Whole year	21.6	22.5	25±4.5
	Apr - Dec	18.6	19.5	24±4.5
STY Genesis	Whole year	7.3	6.1	9.5±3.6
	Apr - Dec	7.3	6.1	9.3±3.4

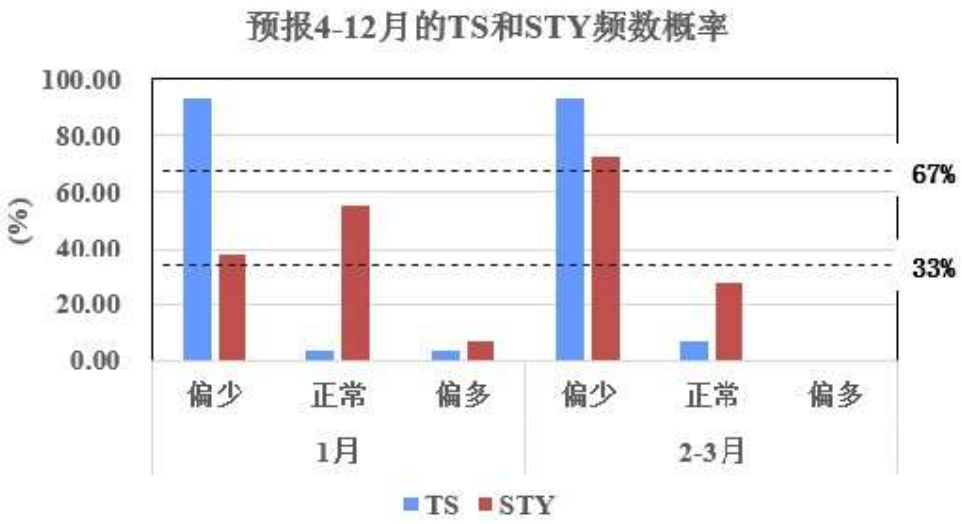

Figure 8. Probabilistic forecasts of TS and STY frequency for April–December 2026 based on the hybrid dynamic–statistical model

4.3. Forecast Results of Dynamical Downscaling Model (iRAM2)

Five CFSv2 forecast fields (initialized at 00:00 UTC on 1, 3, 5, 7, and 9 March 2026) are utilized as driving conditions, combining with the regional model iRAM2 to produce an ensemble dynamical downscaling forecast. The downscaling forecasts are initialized at 00:00 UTC on 20 March 2026. Ensemble members are denoted as E1–E5, where their respective results and the ensemble mean are presented in Table 5. As shown in the table, all ensemble members predict higher TS genesis frequency during April–September in 2026, with an ensemble mean of 27 TSs which is higher than the LTCA of 17.8.

Table 5. April–September TS genesis frequency forecasts based on the iRAM2 dynamical downscaling regional model

Members	E1	E2	E3	E4	E5	Mean	LTCA
TS Frequency	27	23	18	28	24	24	21

5. Tropical Cyclone Disaster Risk Assessment

As noted above, based on the influence of ENSO on TC activity, four analogue years are identified, ranked by similarity as 1959, 1960, 2002, and 2018. The Tropical Cyclone Potential Risk Index is used to demonstrate the potential disaster risk. As shown in Figure 9, the average tropical cyclone potential risk index for 1958–2024 indicates that disaster risk in 1960 and 2018 was higher than the LTCA, while disaster risk in 1959 and 2002 was slightly lower than the LTCA.

Among the two analogue years with higher disaster risk, 1960 ranks among the most devastating years in terms of typhoon-related disasters since the founding of the People's Republic of China. Typhoon No. 6001, *Mary*, made landfall in Hong Kong and subsequently tracked across eastern region of Guangdong before re-entering the sea near Fujian. Accompanied by storm surge, it caused severe damage in Guangdong, Fujian, and Hong Kong. Record-breaking floods occurred in Guangdong, where some low-lying plains were inundated for 2–4 days. The event resulted in a total of 421 fatalities in Guangdong and Hainan, with 444,700 hectares of crops flooded or damaged. In Fujian Province, 823 villages were inundated with 638 fatalities reported, and 87,000 houses collapsed. In Hong Kong, 30 fatalities were reported, and 150 vessels sank or were damaged. Severe Tropical Storm No. 1818, *Rumbia*, was the most destructive typhoon in terms of disaster losses in 2018, resulting in a widespread heavy to torrential rainfall affected Hebei, Liaoning, Shanghai, Jiangsu, Zhejiang, and surrounding regions. A total of 18.004 million people were affected, with 52 fatalities and direct economic losses of CNY 36.91 billion.

Even in the analogue years with the lowest disaster-inducing risk, extreme TC events cannot be ruled out. Typhoon No. 0205, *Rammasun*, and Typhoon No. 0216, *Sinlaku*, caused maximum wind speeds of 37 m/s and 33 m/s over Dachen Island and Yuhuan county in Zhejiang Province, respectively, with peak gusts reaching 46 m/s, both represented the extreme values of TC intensity for 2002.

Based on impact from analogue historical scenarios, the overall TC disaster risk in 2026 is likely to be higher than LTCA, with the most severe impacts concentrated in South China and East China. Sustained attention should be given to the potential impacts of TCs, particularly extreme events including extreme winds and storm

surges in coastal region. Special emphasis should also be placed on floods and secondary disasters triggered by extreme precipitation and localized short-duration torrential rain.

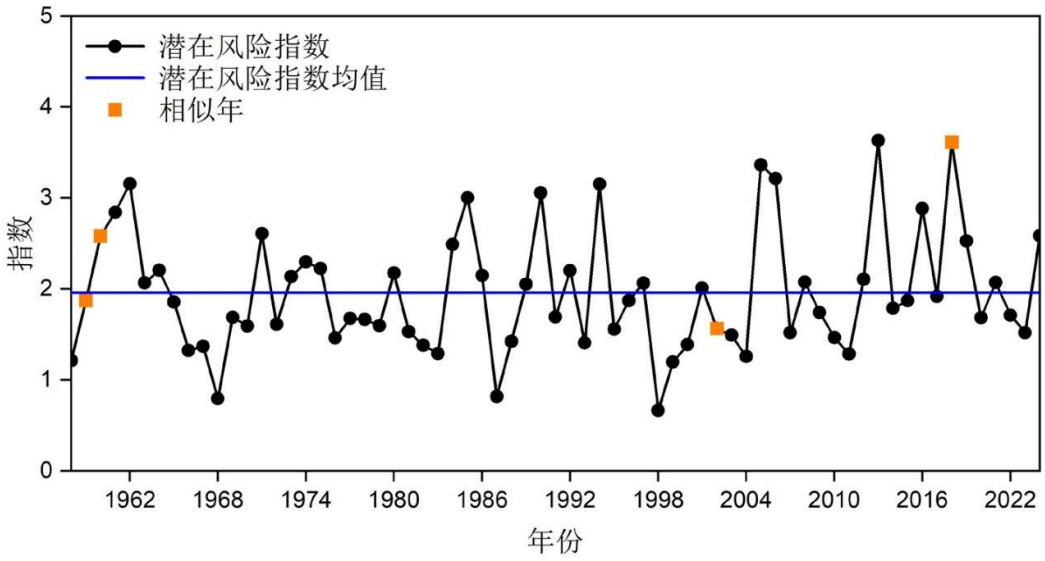

Figure 9. TC potential risk index affecting China during 1958–2024

6. Summary

In conclusion, a weak La Niña condition was observed during the early winter of 2025/26, which decayed in February 2026, and returned to a neutral phase. There is a high probability that will subsequently evolve toward El Niño, some forecasts indicate a transition to El Niño in late spring to early summer, while others forecast a transition in late summer to early autumn.

Dynamic model forecast indicate that anomalous cyclonic circulation is likely to dominate the waters eastern of the Philippines during summer and autumn, providing a favourable condition for TC activity.

Such circulation features show a certain degree of analogous with the regional circulation patterns derived from composite analyses based on historical Niño indices. However, objective forecast methods exhibit discrepancies. Statistical approaches suggest a lower frequency TC activity over the Northwest Pacific and the South China Sea in 2026, whereas dynamic downscaling methods forecast an above-normal TC activity during April–September.

Taking all factors into consideration, TS genesis frequency over the Northwest Pacific and the South China Sea in 2026 is forecasted to be **normal to near normal** LTCA,

while STY frequency slightly below normal LTCA. The frequency of TS making landfall in China will be near the normal LTCA. The frequency of TC that affecting China in 2026 is forecasted to be **at the LTCA**. The frequency of TC affecting South China and East China are forecasted to be above normal to near normal than LTCA; while the frequency of TC affecting areas in the vicinity of Shanghai is close to the LTCA.

Based on impact from analogue historical scenarios, in 2026, typhoon-related disaster risk affecting China is likely to be higher than the LTCA. Sustained attention should be given to the potential impacts of TCs, particularly extreme events including extreme winds and storm surges in coastal region. Special emphasis should also be placed on floods and secondary disasters triggered by extreme precipitation and localized short-duration torrential rain.

Notes:

1. A TC that causes significant impacts is defined as a TC meeting any one of the following criteria:
   (1) At least one station within the region records cumulative precipitation of 50 mm or more during the event; or
   (2) At least one station within the region records sustain wind speeds of Beaufort force 7 or higher, or gusts of Beaufort force 8 or higher; or
   (3) At least one station within the region records cumulative precipitation of 30 mm or more during the event, in conjunction with sustain wind speeds of Beaufort force 6 or higher or gusts of Beaufort force 7 or higher.

2. The South China region refers to Guangdong, Guangxi, and Hainan Provinces. The East China region refers to Fujian, Jiangxi, Zhejiang, Anhui, Shanghai, Jiangsu and Shandong.

3. This document is a free translation of the Chinese report. In case of any discrepancy or ambiguity, the Chinese version shall prevail. For further clarification, please refer to the Chinese report or contact Peak Re staff (Kun Cheng).